

Energetic Constraints on a Rapid Gamma-Ray Flare in PKS 1222+216

Krzysztof Nalewajko,^{1*} Mitchell C. Begelman,^{1,2} Benoît Cerutti,³
Dmitri A. Uzdensky³ and Marek Sikora⁴

¹*JILA, University of Colorado and National Institute of Standards and Technology, 440 UCB, Boulder, CO 80309, USA*

²*Department of Astrophysical and Planetary Sciences, University of Colorado, UCB 389, Boulder, CO 80309, USA*

³*Center for Integrated Plasma Studies, Department of Physics, University of Colorado, UCB 390, Boulder, CO 80309, USA*

⁴*Nicolaus Copernicus Astronomical Centre, Bartycka 18, 00-716 Warsaw, Poland*

13 February 2012

ABSTRACT

We study theoretical implications of a rapid Very-High-Energy (VHE) flare detected by MAGIC in the Flat-Spectrum Radio Quasar PKS 1222+216. The minimum distance from the jet origin at which this flare could be produced is 0.5 pc. A moderate Doppler factor of the VHE source, $\mathcal{D}_{\text{VHE}} \sim 20$, is allowed by all opacity constraints. The concurrent High-Energy (HE) emission observed by Fermi provides estimates of the total jet power and the jet magnetic field strength. Energetic constraints for the VHE flare are extremely tight, requiring a very high co-moving energy density in the emitting region and a very efficient radiative process. We disfavor hadronic processes due to their low radiative efficiency. The External Radiation Compton (ERC) mechanism involving the infrared radiation of the dusty torus is efficient for $\mathcal{D}_{\text{VHE}} \gtrsim 50$. For a magnetic field strength $\gtrsim 0.03 \text{ G} \times (\mathcal{D}_{\text{VHE}}/20)^5$, the Synchrotron Self-Compton (SSC) process dominates the ERC. We consider a scenario involving synchrotron emission by ultra-relativistic electrons accelerated in a magnetic reconnection layer, as has been recently proposed for the case of HE flares in the Crab Nebula. For the case of PKS 1222+216, this mechanism requires an effective electric-to-magnetic field ratio within the layer of $\sim 26 \times (\mathcal{D}_{\text{VHE}}/20)^{-1}$, and a reconnecting magnetic field strength of $\sim 130 \text{ G} \times (\mathcal{D}_{\text{VHE}}/20)^{-3}$. For the origin of an extremely compact emitting region, we prefer a self-collimated jet substructure maintaining its original energy density during propagation to parsec scales, over global jet recollimation by the external medium.

Key words: galaxies: active – quasars: individual: PKS 1222+216 – radiation mechanisms: non-thermal – magnetic reconnection

1 INTRODUCTION

Relativistic jets are responsible for extraordinarily bright emission of blazars that occasionally shows violent variability on a wide range of time scales. The brightest and most rapid flares place the tightest constraints on the source radiative efficiency and energetics. Extremely fast variability of blazars can be probed by telescopes of the highest effective area, i.e. Imaging Atmospheric Cerenkov Telescopes (IACTs), which are sensitive to Very-High-Energy (VHE) photons, $\sim 0.1 - 10 \text{ TeV}$. Two BL Lacertae objects (BL Lacs) were shown to exhibit a variability time scale of a few minutes at an apparent luminosity of the order of $10^{46} \text{ erg s}^{-1}$: PKS 2155-304, observed by H.E.S.S. in July 2006 (Aharonian et al. 2007, 2009; H.E.S.S. Collaboration

2010), and Mrk 501, observed by MAGIC in June and July 2005 (Albert et al. 2007). These flares must be produced in emitting regions smaller than the characteristic size of supermassive black holes producing the jets. This source compactness poses several challenges, including a strong constraint on the minimum energy density and a very high Doppler factor in order to avoid the absorption of VHE gamma rays (Begelman et al. 2008).

Equally surprising were detections of a handful of blazars belonging to the subclass of Flat-Spectrum Radio Quasars (FSRQs) at VHE energies. This is because their VHE emission is expected to be absorbed both internally, if produced within the Broad-Line Region (BLR) with characteristic radius of $\sim 0.1 - 0.3 \text{ pc}$, and externally, if the source is located at a redshift higher than a certain limit depending on the exact energy of observed photons and on the particular model of the Extragalactic Background Light (EBL).

* E-mail: knalew@jila.colorado.edu

3C 279 was detected by MAGIC in early 2006 (Albert et al. 2008) and, at redshift 0.536, remains the most distant known VHE source. PKS 1510-089 was observed by H.E.S.S. in March 2010 (Wagner & Behera 2010), while PKS 1222+216 was detected by MAGIC in June 2010 (Aleksić et al. 2011). The last observation is particularly interesting, because the VHE flux is variable on the time scale of ~ 10 minutes. Thus, the case of PKS 1222+216 combines the difficulties posed by rapid flux variability and a strong radiative environment. This is the first evidence that extremely fast VHE variability in blazars can originate at the parsec scale.

Aleksić et al. (2011) noted that the simultaneous requirements for a very small source radius and its relatively distant location from the jet origin pose a serious challenge. They briefly proposed several alternative solutions, including localized emitting sites or very efficient jet recollimation. Tavecchio et al. (2011) studied the origin of the VHE emission in greater detail, in particular by fitting a two-zone emission model to the broad-band Spectral Energy Distribution (SED) of PKS 1222+216. They adopted a very high Doppler factor of 75 for the compact ‘blob’ producing the VHE flare, but rejected the possibility that it could result from bulk acceleration in a magnetic reconnection site in the ‘minijets’ scenario (Giannios et al. 2009; Nalewajko et al. 2011) because of low expected jet magnetization at parsec scales. With a very high Doppler factor, they strongly favored the External Radiation Compton (ERC) mechanism over Synchrotron Self-Compton (SSC) in their interpretation of the VHE emission. They concluded that the most likely explanation of the rapid VHE flare in PKS 1222+216 is extreme jet focusing due to a recollimation shock in the scenario proposed originally by Bromberg & Levinson (2009).

In this work, we investigate the energetic constraints on the source of the VHE flare in PKS 1222+216 and examine the ability of various radiative processes to explain this phenomenon. In Section 2, we explore the observational constraints, calculate contributions of different radiation components to the gamma-ray opacity, and estimate the jet magnetic field strength. In Section 3, we derive the energetic constraints that need to be satisfied regardless of the radiative mechanism involved. In Section 4, we compare the radiative efficiencies of several processes: ERC, SSC, electron synchrotron, proton synchrotron and photo-meson. In Section 5, we discuss all the constraints and evaluate possible interpretations of this flare. Our results are summarized in Section 6.

The Lorentz factor is $\Gamma = (1 - \beta^2)^{-1/2}$ and the Doppler factor is $\mathcal{D} = [\Gamma(1 - \beta \cos \theta_{\text{obs}})]^{-1}$, where $\beta = v/c$ is the dimensionless velocity and θ_{obs} is the viewing angle. We distinguish between the jet Lorentz factor Γ_j and the VHE emission source Lorentz factor Γ_{VHE} , as well as between the corresponding Doppler factors. We denote quantities measured in the jet co-moving frame with ‘ \prime ’, and those measured in the VHE emitter co-moving frame with ‘ $\prime\prime$ ’. We will refer to Doppler factors satisfying $\mathcal{D}_{\text{VHE}} \sim \Gamma_{\text{VHE}} \sim \Gamma_j \sim 20$ as “typical” and those of $\mathcal{D}_{\text{VHE}} \sim \Gamma_{\text{VHE}} \gg 20$ as “high”. Particle energies are denoted by \mathcal{E} , and electric field strengths by E . Symbols with a numerical subscript should be read as a dimensionless number $X_n = X/(10^n \text{ cgs units})$. We adopt the standard cosmology with $H_0 = 71 \text{ km s}^{-1} \text{ Mpc}^{-1}$, $\Omega_m = 0.27$ and $\Omega_\Lambda = 0.73$.

2 OBSERVATIONAL CONSTRAINTS

PKS 1222+216 (4C +21.35) is located at redshift $z = 0.432$, which corresponds to a luminosity distance of $d_L = 2.4 \text{ Gpc} = 7.3 \times 10^{27} \text{ cm}$. The IACT system MAGIC detected this source on 2010 June 17 (MJD 55364.92) during a 30-min observation (Aleksić et al. 2011). After correction for absorption by the EBL, its spectrum was fitted in the energy range between $\mathcal{E}_{\text{VHE,min,obs}} = 70 \text{ GeV}$ and $\mathcal{E}_{\text{VHE,max,obs}} = 400 \text{ GeV}$ (we adopt a typical photon energy of $\mathcal{E}_{\text{VHE,obs}} \sim 100 \text{ GeV}$) with a power-law model $N(\mathcal{E}) \propto \mathcal{E}^{-\Gamma_{\text{VHE}}}$ with photon index of $\Gamma_{\text{VHE}} = 2.7 \pm 0.3$ and integrated flux of $F_{\text{VHE,obs}} = (2.3 \pm 0.5) \times 10^{-10} \text{ erg s}^{-1} \text{ cm}^{-2}$ (based on their Figure 3), which corresponds to an isotropic luminosity of $L_{\text{VHE}} = 4\pi d_L^2 F_{\text{VHE,obs}} \sim 1.5 \times 10^{47} \text{ erg s}^{-1}$. They were also able to calculate a light curve using 6-min time bins. The first 4 data points show a strong flux increase, with the flux doubling time scale of $t_{\text{VHE,obs}} \sim 10 \text{ min} = 600 \text{ s}$. The last data point indicates a cooling time scale of the same order of magnitude.

Concurrently with the VHE flare, a strong High-Energy (HE; $\sim 0.1 - 10 \text{ GeV}$) flare was observed by the Fermi Large Area Telescope (LAT). The luminosity of the HE flare was $L_{\text{HE}} \sim 10^{48} \text{ erg s}^{-1}$ and the observed variability time scale was crudely estimated at $t_{\text{HE,obs}} \sim 1 \text{ d}$ (Tanaka et al. 2011). A clear spectral break was observed at the energy of $\sim 2 \text{ GeV}$ (with integration time of 8 days), similar to many other bright FSRQs. Such breaks may result from absorption of gamma rays by the ionized helium Ly α continuum (Poutanen & Stern 2010). This would be a strong indication that the HE radiation is produced within the BLR (see Section 5.3). Foschini et al. (2011) presented an independent analysis of the same data, looking for hints of even faster variability. They identified a subflare peaking at MJD 55365.63, 17 h after the MAGIC observation, and estimated the flux rising time scale at $\sim 1.2 \text{ h}$. However, judging from their Figure 3, the flux doubling time scale for this substructure is closer to $\sim 5 \text{ h}$, and the flux troughs are at the level of 50% of the peak flux, putting the significance of this subflare into question. An SED calculated by Foschini et al. (2011) with a 1-day integration time indicates a possible turnover around $\sim 20 \text{ GeV}$.

Optical flux observed in 2010 showed daily variability and moderate linear polarization of $\sim 5\%$, with little correspondence to the gamma-ray flux variations (Smith et al. 2011). This indicates that, while a non-thermal synchrotron component contributes to the optical flux, it is not likely to dominate. VLBI monitoring at 7 mm wavelength (43 GHz) revealed a superluminal component ejected around February/March 2010 (MJD ~ 55260) with apparent propagation velocity of $\sim 14c$ (Jorstad et al. 2011). These authors also report a concurrent rotation of the optical polarization angle by $\sim 200^\circ$.

The low-energy SED of PKS 1222+216 has been analyzed by Tavecchio et al. (2011). With the low level of the synchrotron emission, two thermal components can be clearly identified. The optical/UV spectrum is very hard and appears to be dominated by thermal accretion disk emission of luminosity $L_d \sim 5 \times 10^{46} \text{ erg s}^{-1}$. The IR spectrum indicates the presence of a dusty torus of luminosity $L_{\text{IR}} \sim 10^{46} \text{ erg s}^{-1}$, hence its covering factor is $\xi_{\text{IR}} = L_{\text{IR}}/L_d \sim 0.2$ (Malmrose et al. 2011). They also estimate the covering fac-

tor of the broad-line region at $\xi_{\text{BLR}} \sim 0.02$, hence its luminosity at $L_{\text{BLR}} = \xi_{\text{BLR}} L_d \sim 10^{45} \text{ erg s}^{-1}$. The BLR and the dusty torus form the radiative environment of the jet. From the general knowledge of their properties, we can estimate the energy density profiles of their emission along the jet (see Sikora et al. 2009, for a review). The characteristic BLR radius is

$$r_{\text{BLR}} \sim 0.1 \text{ pc} \times L_{\text{d},46}^{1/2} \sim 0.22 \text{ pc} \sim 7 \times 10^{17} \text{ cm} \quad (1)$$

(Tavecchio & Ghisellini 2008), while the inner radius of the dusty torus for the sublimation temperature of $T_{\text{IR}} \sim 1200 \text{ K}$ is

$$r_{\text{IR}} \sim 4 \text{ pc} \times L_{\text{d},46}^{1/2} T_{\text{IR},3}^{-2.6} \sim 5.6 \text{ pc} \sim 1.7 \times 10^{19} \text{ cm} \quad (2)$$

(Nenkova et al. 2008). Within these inner radii, the energy densities in the external frame are roughly uniform and equal to

$$u_{\text{BLR}}(r < r_{\text{BLR}}) \sim \frac{L_{\text{BLR}}}{4\pi r_{\text{BLR}}^2 c} \sim 6 \times 10^{-3} \text{ erg cm}^{-3}; \quad (3)$$

$$u_{\text{IR}}(r < r_{\text{IR}}) \sim \frac{L_{\text{IR}}}{4\pi r_{\text{IR}}^2 c} \sim 9 \times 10^{-5} \text{ erg cm}^{-3}. \quad (4)$$

The typical energy of photons emitted from the BLR is $\mathcal{E}_{\text{BLR}} \sim \mathcal{E}_{\text{Ly}\alpha} \sim 10 \text{ eV}$ and that of the IR photons $\mathcal{E}_{\text{IR}} \sim 3k_{\text{B}}T_{\text{IR}} \sim 0.3 \text{ eV}$.

Blazar jets have opening angles that generally satisfy the relation $\theta_j \lesssim 1/\Gamma_j$ (Pushkarev et al. 2009). We use it to estimate the typical jet radius at a given distance r from the supermassive black hole:

$$R'_j(r) \sim \frac{r}{\Gamma_j} \sim 8 \times 10^{16} \text{ cm} \times \left(\frac{r}{r_{\text{min}}}\right) \left(\frac{\Gamma_j}{20}\right)^{-1}, \quad (5)$$

where $r_{\text{min}} \sim 0.5 \text{ pc}$ is the minimum distance required to avoid the absorption of gamma rays by the broad emission lines (see Section 2.1). The extremely short variability time scale of the VHE flare introduces a very tight constraint on the size of the VHE emitting region. Its maximum radius and opening angle are

$$R''_{\text{VHE}} \sim \frac{D_{\text{VHE}} c t_{\text{VHE,obs}}}{(1+z)} \sim 2.5 \times 10^{14} \text{ cm} \times \left(\frac{D_{\text{VHE}}}{20}\right), \quad (6)$$

$$\theta_{\text{VHE}} \sim \frac{R''_{\text{VHE}}}{r} \sim 1.7 \times 10^{-4} \left(\frac{D_{\text{VHE}}}{20}\right) \left(\frac{r}{r_{\text{min}}}\right)^{-1}, \quad (7)$$

respectively. The variability time scale of the HE flare constrains the size of the HE emitting region to

$$R'_{\text{HE}} \sim \frac{D_j c t_{\text{HE,obs}}}{(1+z)} \sim 4 \times 10^{16} \text{ cm} \times \left(\frac{D_j}{20}\right), \quad (8)$$

which corresponds to jet distance $r_{\text{HE}} \sim \Gamma_j R'_{\text{HE}} \sim 0.23 \text{ pc} \times (D_j/20)^2 (D_j/\Gamma_j)^{-1}$, almost identical to r_{BLR} . This is consistent with the evidence from the GeV-scale spectral breaks that the HE radiation is produced within the BLR.

2.1 Opacity for gamma rays

The external radiation can absorb gamma-rays produced within the jet in the photon-photon pair production process. This process operates between an absorbed (“hard”) photon of energy $\mathcal{E}_{\text{hard}}$ and an absorbing (“soft”) photon of energy $\mathcal{E}_{\text{soft}}$ when $\mathcal{E}_{\text{hard}}\mathcal{E}_{\text{soft}}/(m_e c^2)^2 > 1$. The peak cross section for this process, $\sigma_{\gamma\gamma} \sim 0.2\sigma_{\text{T}}$, where σ_{T} is the Thomson

cross section, is achieved for $\mathcal{E}_{\text{hard}}\mathcal{E}_{\text{soft}}/(m_e c^2)^2 \sim 3.6$. The IR radiation can absorb hard photons of observed energy

$$\mathcal{E}_{\text{hard,IR,obs}} \gtrsim \frac{(m_e c^2)^2}{(1+z)\mathcal{E}_{\text{IR}}} \sim 600 \text{ GeV}, \quad (9)$$

which is beyond the energy range of the MAGIC observation. For the BLR radiation, the observed threshold is

$$\mathcal{E}_{\text{hard,BLR,obs}} \gtrsim \frac{(m_e c^2)^2}{(1+z)\mathcal{E}_{\text{BLR}}} \sim 18 \text{ GeV}. \quad (10)$$

The optical depth to gamma-ray photons can be as high as $\tau_{\gamma\gamma,\text{BLR}} = \sigma_{\gamma\gamma} n_{\text{BLR}} r_{\text{BLR}} \sim 32$, where $n_{\text{BLR}} = u_{\text{BLR}}/\mathcal{E}_{\text{BLR}}$ is the number density of the BLR photons within r_{BLR} . Thus, if the gamma-ray emission is produced within the BLR, we would expect strong absorption features in the observed SED. However, in PKS 1222+216 there is no evidence for absorption by hydrogen Ly α photons between the MAGIC spectrum and the quasi-simultaneous Fermi/LAT spectrum (Aleksić et al. 2011, although see Section 5.3). The minimum distance r_{min} of the VHE source from the central black hole can be estimated from the dependence of the Ly α absorption threshold on the scattering angle. The minimum scattering angle is given by

$$\chi_{\text{min}} = \arccos \left[1 - \frac{2(m_e c^2)^2}{(1+z)\mathcal{E}_{\text{VHE,max,obs}}\mathcal{E}_{\text{BLR}}} \right] \sim 25^\circ. \quad (11)$$

For the idealized case of a flat BLR contained within the accretion plane, which minimizes r_{min} , and the jet coincident with the BLR symmetry axis, we can simply write $r_{\text{min}} \sim r_{\text{BLR}}/\tan \chi_{\text{min}} \sim 0.5 \text{ pc}$. This estimate should be increased if the BLR emission profile has a significant ‘tail’ for $r > r_{\text{BLR}}$, or if the BLR is extended vertically. Nevertheless, we can safely state that the VHE emission detected by MAGIC is produced at least at the parsec scale.

In this work, we adopt the view that the VHE emission is produced in a tiny region within a broader conical jet, which is similar to the approach of Tavecchio et al. (2011). The remaining volume of the jet may be responsible for the broad-band emission characterizing the quiet state. We should then check whether the jet emission can absorb the gamma-ray photons. Such absorption should be calculated in the jet co-moving frame, where the soft photons are approximately isotropic. Hence, the observed energy of the soft photons is

$$\mathcal{E}_{\text{soft,j,obs}} \sim \frac{3.6(D_j m_e c^2)^2}{(1+z)^2 \mathcal{E}_{\text{VHE,obs}}} \sim 1.8 \text{ keV} \times \left(\frac{D_j}{20}\right)^2, \quad (12)$$

which falls into the X-ray band. We place an observational constraint on the luminosity of the soft radiation $L_{\text{soft}} \lesssim L_{\text{X}}$, where $L_{\text{X}} \sim 10^{45} \text{ erg s}^{-1}$ is the X-ray luminosity of PKS 1222+216 measured by Swift (Tavecchio et al. 2011). We also assume that the jet emitting region is stationary in the external frame. A general prescription for calculating the co-moving radiation energy density in such a case is given in Appendix C of Nalewajko et al. (2011). For a spherical geometry of the soft radiation source in the external frame, we find:

$$u'_{\text{soft}} \sim \frac{3 \ln(2\Gamma_j) L_{\text{soft}}}{4\pi c \Gamma_j D_j^3 R_j'^2}. \quad (13)$$

The optical depth to gamma-ray photons in the co-moving frame is

$$\begin{aligned}\tau_{\gamma\gamma,j} &= \sigma_{\gamma\gamma} n'_{\text{soft}} R'_j \sim \frac{3 \ln(2\Gamma_j) \sigma_T L_{\text{soft}}}{20\pi c(1+z) \mathcal{D}_j^2 r \mathcal{E}_{\text{soft},j,\text{obs}}} \sim \\ &\sim 1.5 \times 10^{-3} \times L_{\text{soft},45} \left(\frac{\mathcal{D}_j}{20}\right)^{-2} \left(\frac{r}{r_{\text{min}}}\right)^{-1},\end{aligned}\quad (14)$$

where $n'_{\text{soft}} = u'_{\text{soft}}/\mathcal{E}'_{\text{soft},j}$ is the number density of soft photons in the co-moving frame. We find that absorption of the VHE photons by emission produced in the broader jet is negligible.

For the sake of completeness, we should also consider absorption of gamma rays by the soft radiation co-produced within the VHE source. This soft radiation would be observed at energies

$$\mathcal{E}_{\text{soft,VHE,obs}} \sim \frac{3.6(\mathcal{D}_{\text{VHE}} m_e c^2)^2}{(1+z)^2 \mathcal{E}_{\text{VHE,obs}}} \sim 1.8 \text{ keV} \times \left(\frac{\mathcal{D}_{\text{VHE}}}{20}\right)^2. \quad (15)$$

For $\mathcal{D}_{\text{VHE}} \sim \mathcal{D}_j$, this is obviously the same result as in the previous case. The optical depth inflicted by this internal radiation is

$$\begin{aligned}\tau_{\gamma\gamma,\text{VHE}} &\sim \sigma_{\gamma\gamma} n''_{\text{soft}} R''_{\text{VHE}} \sim \\ &\sim \frac{\sigma_T L_{\text{soft}}}{20\pi c(1+z) \mathcal{D}_{\text{VHE}}^3 R''_{\text{VHE}} \mathcal{E}_{\text{soft,VHE,obs}}} \sim \\ &\sim 0.04 \times L_{\text{soft},45} \left(\frac{\mathcal{D}_{\text{VHE}}}{20}\right)^{-6}.\end{aligned}\quad (16)$$

Here, we use the co-moving energy density valid for a moving source:

$$u''_{\text{soft}} \sim \frac{L_{\text{soft}}}{4\pi c R_{\text{VHE}}'^2} \sim \frac{L_{\text{soft}}}{4\pi c \mathcal{D}_{\text{VHE}}^4 R_{\text{VHE}}'^2}. \quad (17)$$

If we instead chose a transformation for a stationary source, as in the previous case, the resulting optical depth would increase by a factor of $\sim 3 \ln(2\Gamma_{\text{VHE}})$, which value is ~ 11 for $\Gamma_{\text{VHE}} = 20$, and ~ 14 for $\Gamma_{\text{VHE}} = 50$. Hence, the optical depth is below unity even if the VHE source is stationary. The fact that the internal absorption of the VHE emission is insignificant for $\mathcal{D}_{\text{VHE}} \sim 20$ appears to be in conflict with the work of Begelman et al. (2008). We discuss this issue in Section 5.1.3.

2.2 Magnetic field strength

The magnetic field strength can be estimated by modeling the broad-band SED of quasars in the External Radiation Compton (ERC) scenario (see Section 4.1.1). The Compton dominance parameter is defined as the luminosity ratio of the ERC and synchrotron components, $q = L_{\text{ERC}}/L_{\text{SYN}}$. When the Compton scattering is in the Thomson regime, we have $q \sim u'_{\text{ext}}/u'_B$, where u'_{ext} is the energy density of external radiation, while $u'_B = B'^2/(8\pi)$ is the magnetic energy density. For PKS 1222+216, we can use the HE emission, which dominates the overall SED, and the optical emission, which is produced mainly by the thermal component from the accretion disk with a small contribution from the synchrotron component. From the SED compiled by Tavecchio et al. (2011), we estimate the Compton dominance parameter at $q \sim 100$. Since the HE emission is most likely produced within the BLR, we write

$$B'_j \sim \Gamma_j \left(\frac{8\pi u_{\text{BLR}}}{q}\right)^{1/2} \sim 0.75 \text{ G} \times q_2^{-1/2} \left(\frac{\Gamma_j}{20}\right). \quad (18)$$

The distance at which this estimate is made is essentially r_{BLR} . If the magnetic field is dominated by the toroidal component, which is generally thought to be the case at the parsec scale, the magnetic field strength should depend on the location in the jet as $B'_j \propto r^{-1}$. Hence, the magnetic field strength at the distance of 1 pc is $B'_j(1 \text{ pc}) \sim 0.17 \text{ G}$. The Poynting flux corresponding to this value is

$$\begin{aligned}L_B &\sim (\pi R_j'^2)(\Gamma_j^2 u'_{B,j})c \sim \\ &\sim 10^{45} \text{ erg s}^{-1} \times \left(\frac{B'_j r}{0.17 \text{ G pc}}\right)^2 \left(\frac{r}{\Gamma_j R'_j}\right)^{-2}.\end{aligned}\quad (19)$$

A more direct method for estimating the magnetic field strength is based on VLBI measurements of the shift in the absolute position of the radio core as a function of the observing frequency. Typical results at the distance of 1 pc are 0.1 – 0.3 G (*e.g.*, O'Sullivan & Gabuzda 2009). Although we know of no such results for PKS 1222+216, these values are consistent with the one that we calculated for PKS 1222+216 from the Compton dominance.

We note that Tavecchio et al. (2011) adopted a different jet Lorentz factor of $\Gamma_j \sim 10$ and a distance of the HE emitting region that corresponds to $B'_j(1 \text{ pc}) \sim 0.035 \text{ G}$, which is a factor of ~ 5 lower than the value adopted in this work.

3 ENERGETIC CONSTRAINTS

In this section, we discuss energetic constraints on a generic radiative process involving ultra-relativistic particles, that need to be satisfied in order to explain the VHE flare in PKS 1222+216. Let $\mathcal{E}''_{1\text{part}}$ be the particle energy required to produce a spectral component peaking at $\mathcal{E}_{\text{VHE,obs}}$, and $L''_{1\text{part,em}}$ be the emission luminosity of a single such particle, both measured in the co-moving frame of the VHE source. The co-moving cooling time scale is $t''_{\text{cool}} = \mathcal{E}''_{1\text{part}}/L''_{1\text{part,em}}$, and the cooling ratio can be defined as $Q = t''_{\text{VHE}}/t''_{\text{cool}} = R''_{\text{VHE}} L''_{1\text{part,em}}/(\mathcal{E}''_{1\text{part}} c)$, where $t''_{\text{VHE}} = R''_{\text{VHE}}/c$ is the co-moving light-crossing time scale of the emitting region. The total energy carried by the emitting particles should not exceed the total energy content in the emitting region or the total energy that can be supplied through the region boundaries. Thus, we can adopt two different approaches to the problem of energetics: an instantaneous energy release without particle re-energization, or a sustained emission powered by the energy influx.

In the first approach, we first need to calculate the number of emitting particles N_{part} required to explain the total co-moving luminosity L''_{VHE} . For this, we need to know an average observed co-moving luminosity of a single particle $\langle L''_{1\text{part,obs}} \rangle$, so we can write $N_{\text{part}} \sim L''_{\text{VHE}}/\langle L''_{1\text{part,obs}} \rangle$. The relation between $\langle L''_{1\text{part,obs}} \rangle$ and $L''_{1\text{part,em}}$ depends on the cooling ratio. For $Q \ll 1$, we expect $\langle L''_{1\text{part,obs}} \rangle \sim L''_{1\text{part,em}}$. However, for $Q \gg 1$, the observed luminosity will be diluted by the light-travel delays of the order of t''_{VHE} introduced by the causality requirement, hence $\langle L''_{1\text{part,obs}} \rangle \sim (t''_{\text{cool}}/t''_{\text{VHE}}) L''_{1\text{part,em}} \sim L''_{1\text{part,em}}/Q$. Effectively, we can write $\langle L''_{1\text{part,obs}} \rangle \sim L''_{1\text{part,em}}/\max\{Q, 1\}$. Now, using the number of emitting particles, we can calculate their co-moving energy density $u''_{\text{part}} \sim N_{\text{part}} \mathcal{E}''_{1\text{part}}/V''_{\text{VHE}}$, where

V''_{VHE} is the co-moving volume of the emitting region. We relate this particle energy density to the total co-moving jet energy density

$$u''_{j,\text{VHE}} \sim \frac{u''_{\text{part}}}{\eta_{\text{diss,VHE}}} \sim \frac{\max\{Q, 1\}}{Q} \left(\frac{L''_{\text{VHE}} R''_{\text{VHE}}}{\eta_{\text{diss,VHE}} c V''_{\text{VHE}}} \right), \quad (20)$$

where $\eta_{\text{diss,VHE}} < 1$ is the energy dissipation efficiency, here understood as a fraction of the total jet energy density transferred into the relativistic particles producing the VHE emission. A typical value for the average dissipation efficiency in blazars is $\eta_{\text{diss,VHE}} \sim 0.1$ (e.g., Celotti & Ghisellini 2008).

In the second approach, the total co-moving luminosity L''_{VHE} is constrained by the energy inflow through the boundaries of the emitting region $\dot{\mathcal{E}}''_{\text{in}} \sim u''_j(\beta_{\text{in}} c) A''_{\text{VHE}}$, where β_{in} is the dimensionless inflow velocity and A''_{VHE} is the effective co-moving surface area of the emitting region boundary. The energy dissipation rate related to the VHE emission is $\dot{\mathcal{E}}''_{\text{diss}} = \eta_{\text{diss,VHE}} \dot{\mathcal{E}}''_{\text{in}}$. The relation between L''_{VHE} and $\dot{\mathcal{E}}''_{\text{diss}}$ also depends on the cooling ratio. For $Q \gg 1$, all of the supplied energy can be immediately radiated away and thus we expect $L''_{\text{VHE}} \sim \dot{\mathcal{E}}''_{\text{diss}}$. For $Q \ll 1$, only the Q fraction of the supplied energy can be radiated away, hence $L''_{\text{VHE}} \sim Q \dot{\mathcal{E}}''_{\text{diss}}$. Effectively, we write $L''_{\text{VHE}} \sim \min\{Q, 1\} \dot{\mathcal{E}}''_{\text{diss}}$, from which we find an estimate of the jet energy density:

$$u''_{j,\text{VHE}} \sim \frac{1}{\min\{Q, 1\}} \left(\frac{L''_{\text{VHE}}}{\eta_{\text{diss,VHE}} \beta_{\text{in}} c A''_{\text{VHE}}} \right). \quad (21)$$

Comparing Equations (20) and (21), we immediately notice a close correspondence between them. The dependence of $u''_{j,\text{VHE}}$ on Q is the same in both cases, since $\min\{Q, 1\} \times \max\{Q, 1\} = Q$ is a tautology. We define the radiative efficiency as $\eta_{\text{rad}} \equiv \min\{Q, 1\}$. The geometric factors are $R''_{\text{VHE}}/V''_{\text{VHE}}$ and $1/A''_{\text{VHE}}$, respectively. Their ratio is a dimensionless constant that depends on the choice of a particular shape of the emitting region and on the energy inflow structure. For a spherical geometry and an isotropic energy inflow, we have $V''_{\text{VHE}} = (4/3)\pi R''_{\text{VHE}}{}^3$, $A''_{\text{VHE}} = 4\pi R''_{\text{VHE}}{}^2$, and $R''_{\text{VHE}} A''_{\text{VHE}}/V''_{\text{VHE}} = 3$. The main difference between the two approaches for energetics comes from the introduction of β_{in} in Equation (21), which makes the constraint derived from the energy inflow potentially stronger. This means that a flare that efficiently converts the total energy content available within the emitting region cannot be sustained over time scale longer than t''_{VHE} , unless $\beta_{\text{in}} \sim 1$. This factor is especially limiting in the case of magnetic reconnection, where we expect $\beta_{\text{in}} \lesssim 0.1$ (see Section 4.2.1). However, since the VHE flare observed by MAGIC in PKS 1222+216 is very short, we have no reason to require that this flare be sustained. For the purpose of general considerations in this section, we will adopt the first approach and we will further elaborate the constraint given by Equation (20).

We will now relate the total co-moving luminosity L''_{VHE} to the luminosity observed in the external frame L_{VHE} . The apparent luminosity in the external frame may be affected by two effects: a relativistic boost by a factor of $\mathcal{D}_{\text{VHE}}^4$, and a geometric boost, due to the particle anisotropy in the co-moving frame, by a factor of $4\pi/\Omega''_e$, where Ω''_e is the solid angle covered by the particle beam. Hence, we write $L_{\text{VHE}} \sim (4\pi/\Omega''_e) \mathcal{D}_{\text{VHE}}^4 L''_{\text{VHE}}$. Using this and adopting a spherical geometry, we can calculate the energy density

within the VHE source as

$$u''_{j,\text{VHE}} \sim \frac{1}{\eta_{\text{diss,VHE}} \eta_{\text{rad}}} \left(\frac{\Omega''_e}{4\pi} \right) \left(\frac{3L_{\text{VHE}}}{4\pi c \mathcal{D}_{\text{VHE}}^4 R''_{\text{VHE}}{}^2} \right) \sim \frac{1200 \text{ erg cm}^{-3}}{\eta_{\text{diss,VHE},-1} \eta_{\text{rad}}} \left(\frac{\Omega''_e}{4\pi} \right) \left(\frac{\mathcal{D}_{\text{VHE}}}{20} \right)^{-6}. \quad (22)$$

We call this relation the *Local Energetic Constraint* (LEC). If the jet energy density is homogeneous across the jet radius R'_j , we can relate $u''_{j,\text{VHE}}$ to the total jet power:

$$L_{j,\text{VHE,LEC}} \sim (\pi R_j'^2) (\Gamma_{\text{VHE}}^2 u''_{j,\text{VHE}}) c \sim \frac{3L_{\text{VHE}}}{4\eta_{\text{diss,VHE}} \eta_{\text{rad}}} \left(\frac{\Omega''_e}{4\pi} \right) \left(\frac{\Gamma_{\text{VHE}}^2}{\mathcal{D}_{\text{VHE}}^4} \right) \times \left(\frac{R'_j}{R''_{\text{VHE}}} \right)^2 \sim \frac{2.5 \times 10^{50} \text{ erg s}^{-1}}{\eta_{\text{diss,VHE},-1} \eta_{\text{rad}}} \times \left(\frac{\Omega''_e}{4\pi} \right) \left(\frac{\mathcal{D}_{\text{VHE}}}{20} \right)^{-6} \left(\frac{\Gamma_{\text{VHE}}}{\Gamma_j} \right)^2 \times \left(\frac{R'_j}{r/\Gamma_j} \right)^2 \left(\frac{r}{r_{\text{min}}} \right)^2. \quad (23)$$

This value is certainly too high to be realistic (see Section 5.1.1). There are several ways in which it can be lowered: by increasing the Doppler factor \mathcal{D}_{VHE} , by focusing the emitting particles to a small Ω''_e , or by decreasing the jet radius R'_j . One can also abandon the underlying assumption that the jet is homogeneous across its entire radius.

In the limit of $R'_j \rightarrow R''_{\text{VHE}}$, Equation (23) reduces to what we call the *Global Energetic Constraint* (GEC):

$$L_{j,\text{VHE,GEC}} \sim \frac{3L_{\text{VHE}}}{4\eta_{\text{diss,VHE}} \eta_{\text{rad}}} \left(\frac{\Omega''_e}{4\pi} \right) \left(\frac{\Gamma_{\text{VHE}}^2}{\mathcal{D}_{\text{VHE}}^4} \right) \sim \frac{2.8 \times 10^{45} \text{ erg s}^{-1}}{\eta_{\text{diss,VHE},-1} \eta_{\text{rad}}} \left(\frac{\Omega''_e}{4\pi} \right) \times \left(\frac{\mathcal{D}_{\text{VHE}}}{20} \right)^{-2} \left(\frac{\mathcal{D}_{\text{VHE}}}{\Gamma_{\text{VHE}}} \right)^{-2}. \quad (24)$$

It can be interpreted either as the total jet power required in the case of extreme recollimation or as the fraction of the total jet power associated with the VHE source. It provides a solid lower limit on the total jet. However, since $L_{\text{VHE}} \ll L_{\text{HE}}$, the GEC is even more constraining for the HE flare. Indeed, the GEC may be more relevant to the HE flare, since the variability time scale of the HE emission is consistent with the jet radius in the BLR, where this emission is most likely produced. We can use an analogous formula to that in Equation (24):

$$L_{j,\text{HE}} \sim \frac{3L_{\text{HE}}}{4\eta_{\text{diss,HE}} \eta_{\text{rad}}} \left(\frac{\Omega'_e}{4\pi} \right) \left(\frac{\Gamma_j^2}{\mathcal{D}_j^4} \right) \sim \frac{1.9 \times 10^{46} \text{ erg s}^{-1}}{\eta_{\text{diss,HE},-1} \eta_{\text{rad}}} \left(\frac{\Omega'_e}{4\pi} \right) \left(\frac{\mathcal{D}_j}{20} \right)^{-2} \left(\frac{\mathcal{D}_j}{\Gamma_j} \right)^{-2}. \quad (25)$$

The jet Lorentz factor Γ_j and the dissipation efficiency η_{diss} are unlikely to be significantly higher than 20 and 0.1, respectively, while particle anisotropy is not expected for the HE emission produced in the ERC process. Hence, we accept this value as the best estimate of the total jet power in PKS 1222+216 during the concurrent HE-VHE flares (see also Tanaka et al. 2011). The co-moving jet energy density

associated with the HE flare is

$$\begin{aligned} u'_{j,HE} &\sim \frac{1}{\eta_{\text{diss,HE}}\eta_{\text{rad}}} \left(\frac{\Omega'_e}{4\pi} \right) \left(\frac{3L_{\text{HE}}}{4\pi c D_j^4 R_{\text{HE}}^2} \right) \sim \\ &\sim \frac{0.4 \text{ erg cm}^{-3}}{\eta_{\text{diss,HE},-1}\eta_{\text{rad}}} \left(\frac{\Omega'_e}{4\pi} \right) \left(\frac{D_j}{20} \right)^{-6}. \end{aligned} \quad (26)$$

The fact that $u'_{j,HE} \ll u''_{j,VHE}$, unless the Doppler factor of the VHE source is extremely high, is consistent with the large difference between the jet power estimates $L_{j,HE}$ and $L_{j,VHE,LEC}$. This relation between energy density requirements is remarkable, given that the HE emission should be produced within the BLR, at shorter distances than the VHE emission.

The LEC is weaker than the equipartition condition $u''_{\text{part}} \sim u''_B$ required by some authors (*e.g.*, Böttcher et al. 2009), since the magnetic energy density should satisfy $u''_B < u''_j$. Using the above definitions, equipartition can be formulated as $L_{j,VHE,LEC} \sim L_B$. In fact, the value of L_B given by Equation (19) is more than 5 orders of magnitude lower than the value of $L_{j,VHE,LEC}$.

Since the LEC is extremely tight, it is clear that a high radiative efficiency, with $Q \gtrsim 1$, is critical for the VHE flare energetics. Also, in the case of $Q \ll 1$, VHE emitting particles could spread far outside the VHE source, substantially increasing the observed variability time scale. As we will show in the next section, the $Q \gtrsim 1$ requirement for typical jet parameters is quite demanding.

4 RADIATIVE PROCESSES

Here, we consider various radiative processes in the context of the VHE flare in PKS 1222+216: Inverse Compton (IC) scattering (Section 4.1), in particular External Radiation Compton (ERC, Section 4.1.1) and Synchrotron Self-Compton (SSC, Section 4.1.2); synchrotron radiation (Section 4.2); and hadronic processes (Section 4.3). For each process, we calculate the cooling ratio and provide additional constraints on parameters of the emitting region. These results are compared and summarized in Section 4.4.

4.1 Inverse Compton (IC) scattering

Inverse Compton scattering of soft radiation fields off ultra-relativistic electrons is the most successful model of gamma-ray emission in blazars and many other astrophysical sources. The co-moving energy of electrons that can upscatter soft photons of energy $\mathcal{E}_{\text{soft}}''$ to produce the VHE emission is $\gamma_{e,IC} \sim [(1+z)\mathcal{E}_{VHE,obs}/(\mathcal{D}_{VHE}\mathcal{E}_{\text{soft}}'')]^{1/2}$. The scattering proceeds in the Thomson regime if $b_{\text{soft}} = \gamma_{e,IC}\mathcal{E}_{\text{soft}}''/(m_e c^2) < 1$, which translates to

$$\mathcal{E}_{\text{soft}}'' < \frac{\mathcal{D}_{VHE}(m_e c^2)^2}{(1+z)\mathcal{E}_{VHE,obs}} \sim 36 \text{ eV} \times \left(\frac{\mathcal{D}_{VHE}}{20} \right). \quad (27)$$

In such a case, the luminosity of a single electron is $L''_{1e,IC} \sim \sigma_T c u''_{\text{soft}} \gamma_{e,IC}^2$, where u''_{soft} is the energy density of soft photons, and the cooling ratio is

$$\begin{aligned} Q_{IC} &\sim b_{\text{soft}} \sigma_T n''_{\text{soft}} R''_{VHE} \sim \\ &\sim 17 \left(\frac{\mathcal{D}_{VHE}}{20} \right)^{1/2} \left(\frac{\mathcal{E}_{\text{soft}}''}{1 \text{ eV}} \right)^{-1/2} u''_{\text{soft},0}, \end{aligned} \quad (28)$$

where $n''_{\text{soft}} = u''_{\text{soft}}/\mathcal{E}_{\text{soft}}''$ is the number density of soft photons.

In the context of FSRQs, the most relevant sources of soft radiation for IC scattering are various forms of external radiation (Section 4.1.1) and the local synchrotron radiation (Section 4.1.2).

4.1.1 External Radiation Compton (ERC)

Energy density of the external radiation in the co-moving frame is boosted by a factor of $u''_{\text{ext}}/u_{\text{ext}} \sim \Gamma_{VHE}^2$, while the photon energy increases by a factor of $\mathcal{E}_{\text{ext}}''/\mathcal{E}_{\text{ext}} \sim \Gamma_{VHE}$. Hence, the Thomson limit is $\mathcal{E}_{\text{ext}} < 1.8 \text{ eV} \times (\mathcal{D}_{VHE}/\Gamma_{VHE})$ and the cooling ratio for the ERC process is

$$\begin{aligned} Q_{ERC} &\sim 1500 \times u_{\text{ext},0} \left(\frac{\mathcal{D}_{VHE}}{20} \right)^2 \left(\frac{\mathcal{D}_{VHE}}{\Gamma_{VHE}} \right)^{-3/2} \times \\ &\times \left(\frac{\mathcal{E}_{\text{ext}}}{1 \text{ eV}} \right)^{-1/2}. \end{aligned} \quad (29)$$

The main components of external radiation in FSRQs are the broad emission lines and the thermal infrared emission from the dusty torus. Since the gamma-ray opacity arguments constrain the VHE emission to be produced outside the BLR, here we do not consider the ERC(BLR) process, but only the ERC(IR). The IR radiation, with a typical photon energy of $\mathcal{E}_{IR} \sim 0.3 \text{ eV}$, is scattered in the Thomson regime. The electron Lorentz factor required for the ERC(IR) scenario is

$$\gamma_{e,ERC(IR)} \sim 3.5 \times 10^4 \times \left(\frac{\mathcal{D}_{VHE}}{20} \right)^{-1} \left(\frac{\mathcal{D}_{VHE}}{\Gamma_{VHE}} \right)^{1/2}. \quad (30)$$

For a VHE source located within r_{IR} , the cooling ratio is

$$Q_{ERC(IR)} \sim 0.25 \left(\frac{\mathcal{D}_{VHE}}{20} \right)^2 \left(\frac{\mathcal{D}_{VHE}}{\Gamma_{VHE}} \right)^{-3/2}, \quad (31)$$

which is slightly below unity for a typical Doppler factor, but exceeds unity for $\mathcal{D}_{VHE} \gtrsim 40$.

In the presence of magnetic fields, the same electrons that scatter external radiation into the VHE band will also produce some synchrotron radiation, and in turn Comptonize it into Synchrotron Self-Compton (SSC) radiation. Comparing the luminosities of these components to the observed SED of PKS 1222+216 allows us to put constraints on the magnetic field strength. The observed photon energy and luminosity of the synchrotron radiation are (see Section 4.2)

$$\begin{aligned} \mathcal{E}_{\text{SYN,obs}} &\sim 20 \text{ neV} \frac{\mathcal{D}_{VHE} B_0'' \gamma_{e,ERC(IR)}^2}{1+z} \sim \\ &\sim 0.33 \text{ keV} \times B_0'' \left(\frac{\Gamma_{VHE}}{20} \right)^{-1}, \end{aligned} \quad (32)$$

$$\begin{aligned} L_{\text{SYN}} &\sim \left(\frac{u''_B}{u''_{IR}} \right) L_{VHE} \sim \\ &\sim 1.7 \times 10^{47} \text{ erg s}^{-1} \times B_0''^2 \left(\frac{\Gamma_{VHE}}{20} \right)^{-2}, \end{aligned} \quad (33)$$

respectively. Here, $B_0'' = B''/(1 \text{ G})$. For $B_0'' \sim 1$, this component would appear in the soft X-ray band, much stronger than the observed X-ray luminosity of $L_X \sim 10^{45} \text{ erg s}^{-1}$. In order to keep the synchrotron luminosity below L_X , one

needs to satisfy $B'' < 0.08 \text{ G} \times (\Gamma_{\text{VHE}}/20)$. For the SSC radiation, the observed photon energy, the Klein-Nishina threshold and the apparent luminosity are

$$\begin{aligned} \mathcal{E}_{\text{SSC,obs}} &\sim \gamma_{\text{e,ERC(IR)}}^2 \mathcal{E}_{\text{SYN,obs}} \sim \\ &\sim 400 \text{ GeV} \times B_0'' \times \left(\frac{\mathcal{D}_{\text{VHE}}}{20}\right)^{-3} \left(\frac{\mathcal{D}_{\text{VHE}}}{\Gamma_{\text{VHE}}}\right)^2, \end{aligned} \quad (34)$$

$$\begin{aligned} \gamma_{\text{e,SSC,KN}} &\sim \frac{\mathcal{D}_{\text{VHE}} m_e c^2}{(1+z) \mathcal{E}_{\text{SYN,obs}}} \sim \\ &\sim 2.1 \times 10^4 B_0''^{-1} \times \left(\frac{\mathcal{D}_{\text{VHE}}}{20}\right)^2 \left(\frac{\mathcal{D}_{\text{VHE}}}{\Gamma_{\text{VHE}}}\right)^{-1}, \\ L_{\text{SSC}} &\sim \left(\frac{u_{\text{SYN}}''}{u_{\text{IR}}''}\right) L_{\text{VHE}} \sim \frac{L_{\text{SYN}} L_{\text{VHE}}}{4\pi c \mathcal{D}_{\text{VHE}}^4 R_{\text{VHE}}'^2 u_{\text{IR}}''} \sim \\ &\sim 1.9 \times 10^{50} \text{ erg s}^{-1} \times B_0''^2 \left(\frac{\mathcal{D}_{\text{VHE}}}{20}\right)^{-10} \times \\ &\times \left(\frac{\mathcal{D}_{\text{VHE}}}{\Gamma_{\text{VHE}}}\right)^4, \end{aligned} \quad (35)$$

respectively. The IC scattering of the synchrotron photons proceeds in the Thomson regime for $B'' < 0.6 \text{ G} \times (\mathcal{D}_{\text{VHE}}/20)^3 (\mathcal{D}_{\text{VHE}}/\Gamma_{\text{VHE}})^{-3/2}$. The SSC luminosity is below L_{VHE} for

$$B'' < 0.028 \text{ G} \times \left(\frac{\mathcal{D}_{\text{VHE}}}{20}\right)^5 \left(\frac{\mathcal{D}_{\text{VHE}}}{\Gamma_{\text{VHE}}}\right)^{-2}. \quad (36)$$

For a magnetic field strength equal to this limit, the SSC signal would be observed at $\mathcal{E}_{\text{SSC,obs}} \sim 11 \text{ GeV}$, which is within the Fermi/LAT band. It should be noted here that the quasi-simultaneous luminosity at 10 GeV energies could be somewhat higher than L_{VHE} . For typical Doppler factors, the constraint on the magnetic field strength from the SSC luminosity is stronger than the one from the synchrotron luminosity. As we showed in Section 2.2, the expected magnetic field strength at the distance of r_{min} is about one order of magnitude higher than the upper limit from the SSC luminosity. For high Doppler factors, the stronger constraint will be the one from the synchrotron luminosity. In the case of $\mathcal{D}_{\text{VHE}} \sim \Gamma_{\text{VHE}} \sim 50$, the maximum allowed magnetic field strength is $B'' \sim 0.2 \text{ G}$. However, the synchrotron component would then peak at $\mathcal{E}_{\text{SYN,obs}} \sim 26 \text{ eV}$, in the far-UV band, and thus would be subject to severe extinction. In this case, the constraint on the magnetic field strength from the synchrotron luminosity would be insignificant.

4.1.2 Synchrotron Self-Compton (SSC)

The Lorentz factor required to produce SSC emission peaking at VHE energies is¹

$$\begin{aligned} \gamma_{\text{e,SSC}} &\sim \left[\frac{(1+z) \mathcal{E}_{\text{VHE,obs}}}{20 \text{ neV} \times \mathcal{D}_{\text{VHE}} B_0''}\right]^{1/4} \sim \\ &\sim 2.4 \times 10^4 \times B_0''^{-1/4} \left(\frac{\mathcal{D}_{\text{VHE}}}{20}\right)^{-1/4}, \end{aligned} \quad (37)$$

The observed energy of the soft synchrotron radiation is

$$\mathcal{E}_{\text{SYN,obs}} \sim 20 \text{ neV} \frac{\mathcal{D}_{\text{VHE}} B_0'' \gamma_{\text{e,SSC}}^2}{1+z} \sim$$

¹ Here, by “neV” we do mean 10^{-9} eV .

$$\sim 0.17 \text{ keV} \times B_0''^{1/2} \left(\frac{\mathcal{D}_{\text{VHE}}}{20}\right)^{1/2}. \quad (38)$$

The scattering proceeds in the Thomson regime for

$$\begin{aligned} B'' &< \frac{(m_e c^2)^4}{20 \text{ neV G}^{-1}} \left[\frac{\mathcal{D}_{\text{VHE}}}{(1+z) \mathcal{E}_{\text{VHE,obs}}}\right]^3 \sim \\ &\sim 9 \text{ G} \times \left(\frac{\mathcal{D}_{\text{VHE}}}{20}\right)^3, \end{aligned} \quad (39)$$

which is easily satisfied for parsec-scale jets (see Section 2.2). The co-moving energy density of the soft synchrotron radiation is calculated from the relation $L_{\text{VHE}} = L_{\text{SSC}} \sim (u_{\text{SYN}}''/u_{\text{B}}'') L_{\text{SYN}}$:

$$\begin{aligned} u_{\text{SYN}}'' &\sim \frac{B''}{4\pi \mathcal{D}_{\text{VHE}}^2 R_{\text{VHE}}''} \left(\frac{L_{\text{VHE}}}{2c}\right)^{1/2} \sim \\ &\sim 1.3 \text{ erg cm}^{-3} \times B_0'' \left(\frac{\mathcal{D}_{\text{VHE}}}{20}\right)^{-3}. \end{aligned} \quad (40)$$

The cooling ratio of the SSC process is

$$\begin{aligned} Q_{\text{SSC}} &\sim \frac{\sigma_{\text{T}} R_{\text{VHE}}'' u_{\text{SYN}}'' \gamma_{\text{e,SSC}}}{m_e c^2} \sim \\ &\sim 6.3 \times B_0''^{3/4} \left(\frac{\mathcal{D}_{\text{VHE}}}{20}\right)^{-9/4}. \end{aligned} \quad (41)$$

For magnetic fields in the range of $B'' \sim 0.1 - 1 \text{ G}$ and for typical Doppler factors, this cooling ratio is about one order of magnitude higher than for the ERC(IR) process. However, in contrast to the ERC processes, it strongly decreases with increasing Doppler factor.

For consistency, we check the apparent luminosities of the synchrotron and the ERC(IR) components produced by the same electrons:

$$\begin{aligned} L_{\text{SYN}} &\sim \left(\frac{u_{\text{B}}''}{u_{\text{syn}}''}\right) L_{\text{VHE}} \sim \\ &\sim 4.8 \times 10^{45} \text{ erg s}^{-1} \times B_0'' \left(\frac{\mathcal{D}_{\text{VHE}}}{20}\right)^3, \end{aligned} \quad (42)$$

$$\begin{aligned} L_{\text{ERC(IR)}} &\sim \left(\frac{u_{\text{IR}}''}{u_{\text{syn}}''}\right) L_{\text{VHE}} \sim 4.3 \times 10^{45} \text{ erg s}^{-1} \times \\ &\times B_0''^{-1} \left(\frac{\mathcal{D}_{\text{VHE}}}{20}\right)^5 \left(\frac{\mathcal{D}_{\text{VHE}}}{\Gamma_{\text{VHE}}}\right)^{-2}. \end{aligned} \quad (43)$$

Since the synchrotron component would appear in the soft X-ray band, we need to ensure that $L_{\text{SYN}} < L_{\text{X}} \sim 10^{45} \text{ erg s}^{-1}$. From this, we find a constraint on the magnetic field strength: $B'' < 0.21 \text{ G} \times (\mathcal{D}_{\text{VHE}}/20)^{-3}$. The ERC(IR) emission would be observed at the energy

$$\begin{aligned} \mathcal{E}_{\text{ERC(IR),obs}} &\sim 50 \text{ GeV} \times B_0''^{-1/2} \left(\frac{\mathcal{D}_{\text{VHE}}}{20}\right)^{3/2} \times \\ &\times \left(\frac{\mathcal{D}_{\text{VHE}}}{\Gamma_{\text{VHE}}}\right)^{-1}, \end{aligned} \quad (44)$$

which is very close to the MAGIC band. However, unless the magnetic field strength is as low as required by Equation (36), the ERC(IR) component will be fainter than the SSC component.

4.2 Synchrotron radiation

Synchrotron emission from FSRQ blazars usually peaks in the IR band and does not extend beyond the UV band.

This corresponds to maximum electron Lorentz factors of $\gamma_e \sim 10^{3-4}$. The same electrons will also produce an ERC component extending to GeV energies. Electrons of much higher energies will scatter the external radiation very inefficiently, because the scattering will proceed deeply in the Klein-Nishina regime. But their synchrotron emission may extend into the HE band, the evidence for which we find in the flares recently detected in the Crab Nebula (Abdo et al. 2011; Striani et al. 2011; Buehler et al. 2011). If electrons can be accelerated to such extreme energies in blazars, their synchrotron components could extend even beyond the HE band, in part due to the relativistic Doppler effect. Here, we consider the possibility that the VHE emission from PKS 1222+216 is of synchrotron origin.

In order to produce emission observed at VHE energies, we require electrons of Lorentz factor

$$\gamma_{e,\text{SYN}} \sim \left[\frac{(1+z)\mathcal{E}_{\text{VHE,obs}}}{20 \text{ neV} \times \mathcal{D}_{\text{VHE}} B_0''} \right]^{1/2} \sim 6 \times 10^8 \times B_0''^{-1/2} \left(\frac{\mathcal{D}_{\text{VHE}}}{20} \right)^{-1/2}, \quad (45)$$

where the term $20 \text{ neV} = 0.274 \text{ G} \times \hbar c / (m_e c)$ is the characteristic synchrotron photon energy for $B'' = 1 \text{ G}$ and in the limit of $\gamma_e \rightarrow 1$. The luminosity of a single electron is $L_{1e,\text{SYN}} \sim \sigma_T c u_B'' \gamma_{e,\text{SYN}}^2$. The cooling ratio for the synchrotron process is

$$Q_{\text{SYN}} \sim \frac{\sigma_T u_B'' R_{\text{VHE}}'' \gamma_{e,\text{SYN}}}{m_e c^2} \sim 4900 \times B_0''^{3/2} \left(\frac{\mathcal{D}_{\text{VHE}}}{20} \right)^{1/2}. \quad (46)$$

The requirement that $Q_{\text{SYN}} \geq 1$ can be satisfied already for $B'' > 3 \text{ mG} \times (\mathcal{D}_{\text{VHE}}/20)^{-1/3}$. For magnetic field strengths typical of parsec-scale jets, the cooling ratio for the synchrotron process can be 3 orders of magnitude higher than that for the ERC(IR) process.

4.2.1 Extreme electron acceleration

Although the cooling ratio for the synchrotron process in producing the VHE emission is very high, strong radiative losses pose a problem for accelerating electrons to the required energy (*e.g.*, de Jager et al. 1996; Lyutikov 2010; Uzdensky et al. 2011). If the acceleration proceeds in a uniform electric field E'' and a uniform magnetic field B'' , then the maximum electron Lorentz factor allowed by the radiative losses is $\gamma_{e,\text{max}} \sim (6\pi e E'' / \sigma_T)^{1/2} / B_\perp''$, where B_\perp'' is the magnetic field component perpendicular to the electric field. The observed energy of the corresponding synchrotron radiation is

$$\mathcal{E}_{\text{SYN}} \sim 20 \text{ neV G}^{-1} \times \frac{6\pi e \mathcal{D}_{\text{VHE}}}{(1+z)\sigma_T} \left(\frac{E''}{B_\perp''} \right) \sim 4 \text{ GeV} \times \left(\frac{\mathcal{D}_{\text{VHE}}}{20} \right) \left(\frac{E''}{B_\perp''} \right). \quad (47)$$

In order to explain the VHE emission of PKS 1222+216 with synchrotron radiation, we require $E''/B_\perp'' \sim 26(\mathcal{D}_{\text{VHE}}/20)^{-1}$. This condition violates the ideal MHD approximation, $\mathbf{E}'' \sim \mathbf{B}'' \times \boldsymbol{\beta}$. However, it can be satisfied in magnetic reconnection sites, where the MHD limit does not

apply. Kirk (2004) described a mechanism of extreme particle acceleration in magnetic reconnection layers, in which sufficiently energetic electrons follow relativistic Speiser orbits, which tend to focus them into the region located around the layer midplane, where B_\perp'' vanishes, and $E''/B_\perp'' > 1$ locally. This mechanism has been applied successfully to the case of the Crab Nebula flares (Uzdensky et al. 2011; Cerutti et al. 2012). Still, the requirement that $E''/B_\perp'' \sim 26$ is rather severe, as it can only be satisfied in a tiny fraction of the reconnection layer volume. In the scenario applied to the Crab Nebula flares, $E''/B_\perp'' \sim 4$ was sufficient. We would need an extremely high Doppler factor of $\mathcal{D}_{\text{VHE}} \sim 130$ in order to have the same situation in the case of PKS 1222+216.

In a magnetic reconnection layer, the electric field E''_{acc} that accelerates electrons is induced by the reconnecting magnetic field B_{VHE}'' . Therefore, we have $E''_{\text{acc}} \sim \beta_{\text{rec}} B_{\text{VHE}}''$, where $\beta_{\text{rec}} \lesssim 0.1$ is the dimensionless reconnection rate. The magnetic energy cannot be stored within the reconnection layer; instead it needs to be continuously supplied. Thus, the Local Energetic Constraint (LEC) for the case of magnetic reconnection has to be calculated by following the energy inflow approach. Hence, we take Equation (21) and substitute $u_{\text{B,VHE}}''$ for $u_{\text{j,VHE}}''$, and β_{rec} for β_{in} . The effective surface area of a flat double-faced reconnection layer is $A_{\text{VHE}}'' \sim 2\pi R_{\text{VHE}}''^2$. We obtain the following constraint on the jet magnetic field strength:

$$B_{\text{VHE}}'' \gtrsim \left(\frac{\Omega_e'' L_{\text{VHE}}}{\eta_{\text{diss,VHE}} \eta_{\text{rad}} \pi \beta_{\text{rec}} c \mathcal{D}_{\text{VHE}}^4 R_{\text{VHE}}''^2} \right)^{1/2} \sim \frac{130 \text{ G}}{\eta_{\text{rad}}^{1/2}} \Omega_e''^{1/2} \eta_{\text{diss,VHE}}^{-1/2} \beta_{\text{rec,-1}}^{-1/2} \times \left(\frac{\mathcal{D}_{\text{VHE}}}{20} \right)^{-3}. \quad (48)$$

This value is about 3 orders of magnitude higher than what we expect in a parsec-scale jet (see Section 2.2). It can be lowered by one order of magnitude either by increasing the Doppler factor to $\mathcal{D}_{\text{VHE}} \sim 43$ or by decreasing the electron beam solid angle to $\Omega_e'' \sim 0.01 \text{ sr}$. For example, Cerutti et al. (2012) demonstrated that electrons can be focused into a solid angle of $\Omega_e'' \sim 0.1 \text{ sr}$. However, it would require extreme assumptions ($\mathcal{D}_{\text{VHE}} \sim 200$ or $\Omega_e'' \sim 10^{-6} \text{ sr}$) to reconcile the above limit with a plausible jet magnetic field strength of $B_{\text{j}}'(1 \text{ pc}) \sim 0.2 \text{ G}$. As we discuss in Section 5.1.5, a likely interpretation of the VHE flare in PKS 1222+216 may involve a compact, highly magnetized substructure, in which the magnetic field strength may locally satisfy the above limit.

4.3 Hadronic processes

Alternatively to the leptonic IC scenario, many authors consider processes involving ultra-relativistic protons to explain the gamma-ray emission of blazars (*e.g.*, Mannheim 1993; Mücke et al. 2003; Böttcher et al. 2009; Barkov et al. 2010). Here, we calculate cooling ratios for the two most popular hadronic interactions: the proton-synchrotron and photo-meson processes.

The proton-synchrotron process is completely analogous to the electron-synchrotron process. In this context, the only relevant difference between protons and electrons is their mass, with the ratio of $m_p/m_e = 1840$. For a fixed

synchrotron luminosity and peak energy, the cooling ratio of the synchrotron process scales with the particle mass m as $Q_{\text{SYN}} \propto \sigma_T \gamma / m \propto m^{-5/2}$, since $\sigma_T \propto m^{-2}$ and $\gamma \propto m^{1/2}$. Hence, for proton-synchrotron emission we have

$$\gamma_{\text{p,pSYN}} \sim 2.6 \times 10^{10} B_0''^{-1/2} \left(\frac{D_{\text{VHE}}}{20} \right)^{-1/2}, \quad (49)$$

$$Q_{\text{pSYN}} = \left(\frac{m_p}{m_e} \right)^{-5/2} Q_{\text{SYN}} \sim 3 \times 10^{-5} \times B_0''^{3/2} \left(\frac{D_{\text{VHE}}}{20} \right)^{1/2}. \quad (50)$$

In the photo-meson process, protons interact with soft radiation fields, producing pions of rest energy $m_\pi c^2 \sim 140$ MeV that decay and generate leptonic cascades. In order to create a pion in the interaction with a soft photon of energy $\mathcal{E}_{\text{soft}}''$, the proton must have a Lorentz factor satisfying the condition

$$\gamma_{\text{p,p}\gamma} \gtrsim 0.25 \left(2 + \frac{m_\pi}{m_p} \right) \frac{m_\pi c^2}{\mathcal{E}_{\text{soft}}''} \sim 8 \times 10^7 \times \left(\frac{\mathcal{E}_{\text{soft}}''}{1 \text{ eV}} \right)^{-1}. \quad (51)$$

The typical energy of the created pion is $\mathcal{E}_\pi'' \sim \gamma_{\text{p,p}\gamma} m_\pi c^2$. The effective cross-section for this interaction is $\langle \sigma_{\text{p}\gamma} K_{\text{p}\gamma} \rangle \sim 7 \times 10^{-29} \text{ cm}^2$ (Begelman et al. 1990). Hence, the cooling ratio can be estimated as

$$Q_{\text{p}\gamma} \sim \left(\frac{m_\pi}{m_p} \right) \langle \sigma_{\text{p}\gamma} K_{\text{p}\gamma} \rangle R_{\text{VHE}}'' n_{\text{soft}}'' \sim 2.6 \times 10^{-15} \times n_{\text{soft},0}'' \left(\frac{D_{\text{VHE}}}{20} \right), \quad (52)$$

where n_{soft}'' is the number density of soft photons. For the external IR radiation of the dusty torus, the co-moving soft photon energy is $\mathcal{E}_{\text{soft}}'' = \Gamma_{\text{VHE}} \mathcal{E}_{\text{IR}}$ and thus the proton Lorentz factor must satisfy $\gamma_{\text{p,p}\gamma,\text{IR}} \gtrsim 1.25 \times 10^7 (\Gamma_{\text{VHE}}/20)^{-1}$. The co-moving number density of soft photons is

$$n_{\text{soft}}'' = \frac{\Gamma_{\text{VHE}} u_{\text{IR}}}{\mathcal{E}_{\text{IR}}} \sim 4 \times 10^9 \text{ cm}^{-3} \times \left(\frac{\Gamma_{\text{VHE}}}{20} \right), \quad (53)$$

and hence the cooling ratio is

$$Q_{\text{p}\gamma,\text{IR}} \sim 10^{-5} \times \left(\frac{D_{\text{VHE}}}{20} \right)^2 \left(\frac{D_{\text{VHE}}}{\Gamma_{\text{VHE}}} \right)^{-1}. \quad (54)$$

For both processes, we find $Q \ll 1$, even if we assume extremely high values for the Doppler factor and/or the magnetic field strength. We conclude that hadronic processes face serious difficulties in satisfying the energetic requirement for ultra-relativistic protons. This conclusion is in line with a recent review of FSRQ properties by Sikora et al. (2009), and also with the analysis of VHE emission from 3C 279 by Böttcher et al. (2009). In Section 5.2.2, we discuss the model of Barkov et al. (2010), proposed for the fast VHE flares in BL Lac objects, in the context of PKS 1222+216.

4.4 Comparison of radiative processes

The results of this section are summarized in Figure 1. Hadronic processes are much less efficient than leptonic processes, although for the proton-synchrotron process this conclusion depends on the magnetic field strength. The ERC(IR) process is moderately efficient, but for $B'' \gtrsim$

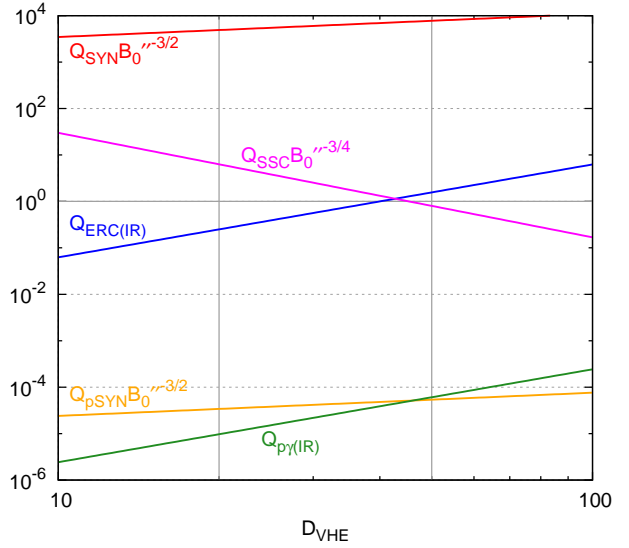


Figure 1. Cooling ratios $Q = t_{\text{VHE}}''/t_{\text{cool}}''$ for all processes considered in Section 4 as functions of the Doppler factor of the VHE source: inverse Compton scattering off the external IR radiation (ERC(IR); blue) or off the local synchrotron radiation (SSC; magenta), electron synchrotron (SYN; red), proton synchrotron (pSYN; orange), and photo-meson scattering off external IR radiation (p γ (IR); green). Cooling ratios for electron and proton synchrotron processes are multiplied by a factor of $B_0''^{-3/2}$, and that for the SSC process is multiplied by a factor of $B_0''^{-3/4}$. The energetic constraints can be satisfied preferentially by radiatively efficient processes with $Q \gtrsim 1$.

$0.03 \text{ G} \times (D_{\text{VHE}}/20)^5$ it will be dominated by the SSC process. While typically in FSRQ blazars the ERC processes are much more efficient than the SSC process (Sikora et al. 2009), in this case the high SSC efficiency is a consequence of an extremely compact emitting region. SSC was favored by Böttcher et al. (2009) as the mechanism of VHE emission in another FSRQ, 3C 279. The synchrotron process is the most efficient of all for $B'' \gtrsim 0.05 \text{ G}$, assuming typical Doppler factors. However, the strong radiative synchrotron losses limit the electron acceleration process in this scenario to the magnetic reconnection sites. Energetic constraints are severe for magnetic reconnection to explain the VHE emission from PKS 1222+216 at the observed luminosity level.

5 DISCUSSION

The flare detected by MAGIC in PKS 1222+216 is an extreme phenomenon that calls for an extreme solution. But it is not our intention to reject the established paradigm of broad-band emission of blazars over longer variability time scales. The entire SED of PKS 1222+216 below 70 GeV has to be explained by a conventional population of electrons with maximum Lorentz factors $\gamma_{\text{e,max}} \sim 10^{3-4}$, producing two spectral components via synchrotron and ERC mechanisms, and most likely filling the entire jet cross section. The evidence for this comes from the relatively long variability time scale of the concurrent HE emission (Tavecchio et al. 2011). As we argue in Section 5.3, the existence of a spectral break at $\sim 2 \text{ GeV}$ implies the existence of another break at

~ 18 GeV, and thus the spectrum measured by MAGIC is unlikely to be an extension of the Fermi/LAT spectrum.

5.1 Local Energetic Constraint

In Section 3, we defined the Local Energetic Constraint (LEC) based on an instantaneous energy content within the emitting region. We also showed that a similar result can be derived by considering the rate of energy inflow through the region's boundaries, if the inflow velocity is close to c . This is not the case for the magnetic reconnection, where the energy inflow rate is limited by the reconnection rate $\beta_{\text{rec}} \lesssim 0.1$. It is unclear whether a flare that satisfies the LEC formulated by Equation (22) can be sustained at the maximum luminosity for a time longer than t_{VHE}'' in any realistic energy dissipation scenario. Nevertheless, this idealized approach to the problem of energetics is very useful in demonstrating that some extreme jet parameters should be adopted. We noted that, independently of the radiative process, we need an extremely high jet power, a very high Doppler factor, a very strong jet collimation and/or a highly anisotropic particle beam in the jet co-moving frame.

5.1.1 Jet power

The total jet power for PKS 1222+216 was estimated by Meyer et al. (2011), who used radio flux measurements at 300 MHz and obtained $L_{\text{j,M11}} \sim 8 \times 10^{44}$ erg s $^{-1}$. This value is not sufficient to satisfy the GEC for the HE flare, since it is smaller than $L_{\text{j,HE}}$, given by Equation (25), by a factor of ~ 24 . It is also slightly lower than the Poynting flux given by Equation (19). Hence, in Section 4, we adopted $L_{\text{j,HE}}$ as the preferred value for the total jet power in PKS 1222+216.

We note that the jet power estimated by Meyer et al. (2011) may not be directly relevant for the extreme VHE flare. Low-frequency radio emission is strongly self-absorbed at parsec scales and hence it can only probe very extended regions. The variability time scale for this emission is of the order of decades, and thus it can only inform us about the jet power averaged over a very long period of time. What was observed in 2010 was an exceptional gamma-ray flare, one of the brightest during the first years of the Fermi mission. If the flare is accompanied by a large increase in the total jet power, the dissipation efficiency η_{diss} at parsec scales could be very high, allowing only a small fraction of the initial jet power to reach larger scales. Furthermore, the duty cycle of such extreme flares may be quite low. For these reasons, episodes of a very large increase in the initial jet power may not contribute substantially to the average jet power at much larger distances. On the other hand, if the jet power increased without a substantial change in the overall dissipation efficiency, we expect that dramatic variations in the resolved radio structure, most likely including the emergence of a bright superluminal radio spot, should follow the 2010 flare (*e.g.*, Savolainen et al. 2002). In fact, a superluminal radio feature was observed with VLBA, with ejection time (defined as the moment of crossing the core corresponding to a synchrotron self-absorption photosphere) estimated at February/March 2010 (Jorstad et al. 2011).

The jet power can be conveniently parametrized with the accretion disk luminosity L_{d} (*e.g.*, Celotti & Ghisellini

2008). Using the typical radiative efficiency of the accretion disk $\eta_{\text{d}} = L_{\text{d}}/(\dot{M}_{\text{acc}}c^2) \sim 0.1$, where \dot{M}_{acc} is the mass accretion rate onto the supermassive black hole, we can calculate the jet production efficiency:

$$\eta_{\text{j}} = \frac{L_{\text{j}}}{\dot{M}_{\text{acc}}c^2} \sim \left(\frac{L_{\text{j}}}{L_{\text{d}}}\right) \eta_{\text{d}} \sim 0.04 \times \eta_{\text{d,-1}} \left(\frac{L_{\text{j}}}{L_{\text{j,HE}}}\right). \quad (55)$$

This value is relatively low, meaning that the jet power $L_{\text{j,HE}}$ adopted in this work is rather modest. Tchekhovskoy et al. (2011) demonstrated by numerical simulations that $\eta_{\text{j}} \gtrsim 1$ is in principle possible. Tanaka et al. (2011) obtained $\eta_{\text{j}} \sim 1$, assuming a lower jet Lorentz factor $\Gamma_{\text{j}} \sim 10$, and a much lower accretion disk luminosity $L_{\text{d}} \sim 5 \times 10^{45}$ erg s $^{-1}$. For $\eta_{\text{j}} \sim 1$, we would expect the jet power to be as high as $L_{\text{j}} \sim 5 \times 10^{47}$ erg s $^{-1}$. This is still lower, by almost 3 orders of magnitude, than the jet power required by the LEC for the VHE flare (see Equation 23).

5.1.2 Jet magnetization

Determination of both the total jet power and the magnetic field strength at a given distance has implications for the average jet magnetization parameter $\sigma_{\text{j}} = B_{\text{j}}'^2/(4\pi w_{\text{j}})$, where w_{j} is the relativistic enthalpy. The total jet energy density $u_{\text{j}}' \sim w_{\text{j}} + u_{\text{B,j}}'$ is related to the total jet power by $L_{\text{j}} \sim (\pi R_{\text{j}}'^2)(\Gamma_{\text{j}}^2 u_{\text{j}}')c$. Using the Poynting flux calculated in Equation (19), we find:

$$\begin{aligned} \frac{\sigma_{\text{j}}}{\sigma_{\text{j}} + 2} \sim \frac{L_{\text{B}}}{L_{\text{j}}} \sim 0.05 \left(\frac{B_{\text{j}}' r}{0.17 \text{ G pc}}\right)^2 \left(\frac{r}{\Gamma_{\text{j}} R_{\text{j}}'}\right)^{-2} \times \\ \times \left(\frac{L_{\text{j}}}{L_{\text{j,HE}}}\right)^{-1}. \end{aligned} \quad (56)$$

This result means that $\sigma_{\text{j}} \sim 0.11$, and thus that the jet is matter-dominated, which is in agreement with the study of Sikora et al. (2005). This magnetization parameter is somewhat lower than those obtained in numerical simulations of jet acceleration (*e.g.*, Komissarov et al. 2009).

5.1.3 Doppler factor

A Lorentz factor of $\Gamma_{\text{VHE}} = 50$ and a Doppler factor of $\mathcal{D}_{\text{VHE}} = 75$ were proposed by Tavecchio et al. (2011) in their interpretation of the VHE flare in PKS 1222+216. Similar relativistic boosts were also suggested for previous cases of fast TeV flares in other blazars (Begelman et al. 2008). Such values for the bulk Lorentz factor are much higher than those inferred from the apparent superluminal motion of individual pc-scale radio features, which typically fall into the 10 – 20 range, with exceptional cases up to ~ 40 (*e.g.* Hovatta et al. 2009). Several solutions to this discrepancy have been proposed, including radiative deceleration (Levinson 2007), the photon breeding mechanism (Stern & Poutanen 2008), stratified jet emission (Boutelier et al. 2008), minijets (Giannios et al. 2009; Nalewajko et al. 2011) and non-steady magnetic acceleration (Lyutikov & Lister 2010). The minijets model postulates that localized relativistic outflows are produced in the jet co-moving frame perpendicularly to the jet bulk motion and powered by Petschek-type magnetic reconnection. However, in order for the minijets to have significant Lorentz factors, the reconnecting plasma must be strongly magnetized, with $\sigma \gg 1$.

In the case of PKS 1222+216, where VHE emission should be produced at $r > r_{\min} \sim 0.5$ pc, the jet plasma should already be matter-dominated (see Section 5.1.2). For this reason, Tavecchio et al. (2011) judged that minijets cannot operate at such large scales. However, in order to achieve an extreme concentration of energy within the VHE source, an efficient magnetic self-collimation mechanism may be required, which would indicate high local magnetization values (see Section 5.1.5). In such a case, the minijets model cannot be excluded.

The main motivation for introducing high Doppler factors of $\mathcal{D}_{\text{VHE}} \sim 50$ in previous cases of fast VHE flares was to avoid the internal absorption of the VHE emission originating in a very compact region (Begelman et al. 2008). In the case of PKS 1222+216, we found insignificant internal absorption for $\mathcal{D}_{\text{VHE}} \sim 20$. The reasons for this apparent inconsistency are the following: the observed photon energy is $\mathcal{E}_{\text{VHE,obs}} \sim 100$ GeV instead of 1 TeV; the soft radiation luminosity is $L_{\text{soft}} \sim 10^{45}$ ergs $^{-1}$ instead of 10^{46} ergs $^{-1}$; the observed variability time scale is $t_{\text{VHE,obs}} \sim 10$ min instead of 5 min; and neglect of the redshift and the 3.6 factor in Equation (15). Different approximations lead to a difference by factor ~ 21 between our Equation (16) and their Equation (16). Even if we drop the 3.6 factor and consider the $\mathcal{E}_{\text{VHE,max,obs}} = 400$ GeV photons, we obtain $\mathcal{E}_{\text{soft,VHE,obs}} \sim 125$ eV $\times (\mathcal{D}_{\text{VHE}}/20)^2$ and $\tau_{\gamma\gamma,\text{VHE}} \sim 0.6 L_{\text{soft},45} (\mathcal{D}_{\text{VHE}}/20)^{-6}$. Hence, the VHE emission in PKS 1222+216 could be produced in a region propagating with a typical Lorentz factor.

A radio element propagating with apparent dimensionless velocity of $\beta_{\text{j,app}} \sim 14$ was detected around the time of the VHE flare (Jorstad et al. 2011). At an earlier epoch, superluminal motion with $\beta_{\text{j,app}} \sim 21$ was reported by Hovatta et al. (2009). These authors also provide an independent estimate of the Doppler factor of $\mathcal{D}_{\text{j}} \sim 5.2$. Combining these two results, they obtain a very high Lorentz factor of $\Gamma_{\text{j}} \sim 46$ and a relatively large viewing angle of $\theta_{\text{obs}} \sim 5.1^\circ$. However, for this combination of a low Doppler factor and a high Lorentz factor, the gamma rays would be strongly absorbed by the soft radiation originating in the jet (see Equation 14). The case of a misaligned jet, with $\theta_{\text{obs}} \sim 4/\Gamma_{\text{j}}$, is not energetically favorable during the 2010 flare of PKS 1222+216, when the apparent broad-band luminosity peaks at the level of $L_{\text{HE}} \sim 10^{48}$ ergs $^{-1}$. If we adopt a fairly probable case of $\theta_{\text{obs}} \sim 1/\Gamma_{\text{j}}$, we expect $\beta_{\text{j,app}} \sim \mathcal{D}_{\text{j}} \sim \Gamma_{\text{j}}$. The estimates made by Hovatta et al. (2009), based on the results of the MOJAVE project, probe the scale of several parsecs over at least a few years. If we accept their estimate of the Lorentz factor, a change in the viewing angle may be explained by jet bending or re-orientation. In fact, Homan et al. (2009) showed a radio component in PKS 1222+216 that propagated along a significantly curved projected trajectory. A change in the orientation of a highly relativistic jet could be the primary driver of the Fermi/LAT flare, although by itself it cannot explain the formation of a very compact region producing the MAGIC flare. Such a scenario has been proposed to explain the optical polarization angle rotation accompanying a major 2009 flare in 3C 279 (Abdo et al. 2010; Nalewajko 2010). It is then interesting that Jorstad et al. (2011) report a rotation of the optical polarization angle by $\sim 200^\circ$, coincident with the high gamma-ray state of PKS 1222+216. On the other hand, if the jet is straight and

does not change its orientation over several years, then our assumption on the viewing angle implies a Lorentz factor of $\Gamma_{\text{j}} \sim 11$. This means that the jet becomes much less relativistic during a major flare, requiring a significant increase in the total jet power to explain the increase in apparent luminosity. As we discussed in Section 5.1.1, such an increase in the total jet power during the flare is supported by the low value of the jet power found in a previous epoch by Meyer et al. (2011). A decrease in the Lorentz factor could be explained by an increase in the mass loading. Nevertheless, we see that a solution to the apparent inconsistency between the low Doppler factor determined by Hovatta et al. (2009) and the requirement for a low gamma-ray optical depth as given by Equation (14) depends strongly on the details of the jet kinematics. Fortunately, our general conclusions are not especially sensitive to our adoption of reference values $\mathcal{D}_{\text{j}} \sim \Gamma_{\text{j}} \sim 20$.

5.1.4 Reconfinement shock nozzle

The opening angle of the VHE emitting region, if located at the broad-line photosphere r_{\min} , is $\sim 1.7 \times 10^{-4}$ (see Equation 7). Aleksić et al. (2011) and Tavecchio et al. (2011) proposed that such a small value can be explained by a reconfinement shock that results from the interaction between the jet and the pressurized external medium. Reconfinement shocks have been proposed as the main dissipation mechanism operating at the scales of a few pc in blazars (Sikora et al. 2008; Nalewajko & Sikora 2009). According to the study by Bromberg & Levinson (2009), reconfinement shocks can focus relativistic jets very efficiently, but this effect depends strongly on the radiative efficiency of the downstream flow. The opening angle inferred in the case of PKS 1222+216 is even smaller than the value of $\sim 5 \times 10^{-4}$ required by the hypothesis that the 2006 TeV flare in M87 originated in the quasi-stationary knot HST-1 (Aharonian et al. 2006; Stawarz et al. 2006). Bromberg & Levinson (2009) considered that hypothesis unrealistic, noting the small radiative efficiency of the M87 jet. For radiative efficiency of 30% they obtained an opening angle of $\sim 3 \times 10^{-3}$. A somewhat larger opening angle of $\sim 6 \times 10^{-3}$ has been obtained for a feature resembling HST-1 in relativistic MHD numerical simulations designed specifically for the case of M87 (Gracia et al. 2009).

These opening angles are more than order of magnitude larger than that required in the case of PKS 1222+216. In Section 2, we found that the observed variability time scale of the HE emission, $t_{\text{HE,obs}} \sim 1$ d, is consistent with the jet being conical, with an opening angle $\sim 1/\Gamma_{\text{j}}$, at least up to the characteristic BLR radius $r_{\text{BLR}} \sim 0.2$ pc. In such a case, jet recollimation may require a distance of several r_{BLR} to complete. The requirement for the initial jet opening angle becomes much more severe if the recollimation nozzle is located even farther away from the jet source. Moreover, the extreme jet focusing mechanism via reconfinement shocks, as proposed by Bromberg & Levinson (2009), depends critically on the assumption of perfect jet axisymmetry. The jet of PKS 1222+216 is certainly not axisymmetric, since individual radio elements were observed to propagate along a curved trajectory (Homan et al. 2009). Hence, the interpretation of the VHE source compactness as due to a reconfinement nozzle is unlikely. However, numerical simulations

(*e.g.*, Gracia et al. 2009) indicate that reconfinement can result in reducing the jet radius by one order of magnitude, as compared to the conical jet, helping to relax the LEC.

5.1.5 Jet substructure

The VHE flare could be associated with the appearance of a very compact and energetic substructure within the jet (*e.g.*, Ghisellini & Tavecchio 2008). This allows one to abandon the LEC and require only that the GEC be satisfied. Should the radius of this substructure correspond to the observed variability time scale of the VHE flare, a substantial fraction of the total jet power, $(L_{j,VHE,GEC}/L_{j,HE}) \sim 15\%$, would be carried through a tiny fraction of the jet cross section, $(R''_{VHE}/R'_j)^2 \sim 10^{-5}$. This extreme requirement could be relaxed somewhat by increasing the Doppler factor \mathcal{D}_{VHE} or by considering an anisotropic co-moving distribution of emitting particles, with $\Omega''_e \lesssim 1$ sr, as expected in the extreme particle acceleration scenario. However, in order to maintain a sharply higher energy density in the substructure, compared to the broad jet, a very efficient self-collimating process must operate. This can be provided by the pinch mechanism, if the structure is highly magnetized. The high magnetization would imply a very strong magnetic field that would be potentially sufficient to power the VHE flare and associated extreme particle acceleration via magnetic reconnection (see Section 4.2.1). High-magnetization regions could be associated with jet cores expected to arise along the axis of the light cylinder (Beskin 2010). Another phenomenon enabled by a high-density magnetized structure propagating through a low-density jet medium is the magnetic rocket effect, in which a thin shell is accelerated to large Lorentz factors, while its magnetization decreases to $\sigma \ll 1$ (Granot et al. 2011). This allows, at least locally, very efficient conversion of Poynting flux to kinetic power. The energy of such an ultra-relativistic but weakly magnetized shell could be efficiently dissipated via fast magnetosonic waves (Komissarov 2012). Such a scenario has been already applied to the fast TeV flares in blazars (Lyutikov & Lister 2010).

5.2 Radiative processes

5.2.1 Synchrotron radiation

Using electron synchrotron radiation to interpret the VHE emission from a blazar would certainly be an unconventional scenario. Although the synchrotron mechanism has by far the highest cooling ratio of all processes considered in Section 4 (for magnetic field strengths of order $B'' \sim 0.2$ G, typical for parsec-scale blazar jets, see Section 2.2), this feature cannot be exploited because of the difficulty in accelerating electrons to the required Lorentz factors $\gamma_{e,SYN} \sim 10^9$. As we showed in Section 4.2.1, in order to avoid severe radiative losses, the acceleration should proceed in the environment where the electric-to-magnetic field strength ratio is $E''/B''_{\perp} \sim 26 \times (\mathcal{D}_{VHE}/20)^{-1}$, which can be satisfied only very deep within a magnetic reconnection layer. This large value by itself poses a serious problem, since it is hard to imagine the focusing mechanism working so perfectly under realistic conditions (Cerutti et al. 2012). Increasing the

source Doppler factor can relax this requirement, but probably not by a large enough factor. Moreover, the typical magnetic field strengths for parsec-scale jets are insufficient by almost 3 orders of magnitude to explain the energetics of the VHE flare. These two problems make the synchrotron scenario for the VHE flare in PKS 1222+216 implausible.

5.2.2 Hadronic processes

Barkov et al. (2010) interpreted the rapid VHE flares in BL Lacs in terms of proton synchrotron emission associated with the interaction between the jet and a red giant star. In order to make the proton synchrotron mechanism efficient, they adopted magnetic field strengths of the order of ~ 100 G and located the emission site at the distance of ~ 0.003 pc from the supermassive black hole. We note that this choice corresponds to a magnetic field strength of ~ 0.3 G at a distance of 1 pc, which is in agreement with typical values (see Section 2.2). From Equation (50), we find that the cooling ratio for the proton synchrotron process, for a magnetic field of ~ 100 G, is $Q_{pSYN} \sim 0.03 \times (\mathcal{D}_{VHE}/20)^{1/2}$. With this value, the jet power required by the GEC for the VHE flare in PKS 1222+216 is $L_{j,VHE,GEC} \sim 9 \times 10^{46} \text{ erg s}^{-1} \times (\mathcal{D}_{VHE}/20)^{-5/2}$ (see Equation 24). This value exceeds the GEC estimate for the HE flare $L_{j,HE}$, which we accepted as the best measure of the total jet power, by a factor of a few. Even if the GEC can be barely satisfied, this particular scenario suffers from a coincidence problem – that a red giant star should be “illuminated” by an extremely narrow energetic beam. In the case of a broader homogeneous jet, we would need to satisfy the LEC and thus assume an extremely high jet power (see Equation 23).

5.3 External gamma-ray opacity

The assumption that the VHE emission must be produced outside the BLR is not as solid as argued by Aleksić et al. (2011) and Tavecchio et al. (2011). The Fermi/LAT spectrum, integrated over longer time intervals around the time of the MAGIC observation, features a break at ~ 2 GeV (Tanaka et al. 2011), which is consistent with absorption due to the He II Ly α continuum (Poutanen & Stern 2010). For the redshift of PKS 1222+216, the threshold for such an absorption process is expected to be observed at $\gtrsim 3.4$ GeV. In such a case, the bulk of the GeV emission should be produced deeply within the BLR. As the He II ions require even higher ionization potential to become excited than the hydrogen atoms, a stronger break due to absorption by the H Ly α photons is expected at $\gtrsim 18$ GeV (see Equation 10). We note that the scattering angle for Ly α absorption cannot be smaller than 90° , if the He II region is nested within the hydrogen ionization region. Because of this additional break, which could not be detected because of limited photon statistics in the Fermi/LAT data above 10 GeV, one should not expect that the Fermi/LAT spectrum above the 2 GeV break can be extended with a power-law all the way to the MAGIC spectrum. The alignment between these two spectra integrated over different time scales may be coincidental, unless the 2 GeV break is not really caused by He II absorption. Therefore, if the observed Fermi/LAT

and MAGIC spectra are produced by different mechanisms, the intrinsic MAGIC spectrum could be significantly harder than the intrinsic Fermi/LAT spectrum above the 2 GeV break. The fact that no absorption feature is observed between 70 GeV and 400 GeV does not exclude a possibility that such a feature exists at lower energies and that the MAGIC spectrum is actually absorbed by the broad emission line photons. While that would allow one to place the emitting region very close to the supermassive black hole, in such a case a much greater intrinsic VHE luminosity would be required.

6 SUMMARY

We studied theoretical implications of a VHE flare of flux-doubling time scale of $t_{\text{VHE,obs}} \sim 10$ min observed by MAGIC at photon energies between 70 GeV and 400 GeV in a FSRQ-class blazar PKS 1222+216. Assuming negligible absorption of the VHE emission by the BLR radiation, we require that its source be located at the distance of at least $r_{\text{min}} \sim 0.5$ pc from the supermassive black hole. The concurrent HE emission is consistent with being produced within the BLR. Contrary to the cases of rapid VHE flares in PKS 2155-304 and Mrk 501, a very high Doppler factor is not implied by the internal gamma-ray opacity argument.

We analyzed energetic constraints that have to be satisfied by any candidate radiative process behind the VHE emission. We formulate the Local Energetic Constraint (LEC), requiring that the energy density of the VHE emitting particles should not exceed the local energy density of the jet, thus estimated at $u''_{\text{j,VHE}} \sim 1200 \text{ erg cm}^{-3} \times (\mathcal{D}_{\text{VHE}}/20)^{-6}$. For a broad homogeneous jet, the LEC calls for an extremely high jet power, $L_{\text{j,VHE,LEC}} \sim 2.5 \times 10^{50} \text{ erg s}^{-1} \times (\mathcal{D}_{\text{VHE}}/20)^{-6}$. A weaker Global Energetic Constraint (GEC), requiring that the total jet power be higher than the power carried by the VHE emitting particles, can be used to estimate the minimum jet power consistent with the VHE emission, $L_{\text{j,VHE,GEC}} \sim 2.8 \times 10^{45} \text{ erg s}^{-1} \times (\mathcal{D}_{\text{VHE}}/20)^{-2}$. In a similar manner, the most likely total jet power can be estimated from the HE luminosity, $L_{\text{j,HE}} \sim 1.9 \times 10^{46} \text{ erg s}^{-1}$. We estimate the total Poynting flux to be $L_{\text{B}} \sim 10^{45} \text{ erg s}^{-1}$.

An efficient radiative process, with a cooling ratio of $Q = t'_{\text{VHE}}/t'_{\text{cool}} \gtrsim 1$, is strongly preferred for the VHE emission. This condition can be satisfied by the ERC(IR) process for $\mathcal{D}_{\text{VHE}} \sim 50$, by the SSC process for $\mathcal{D}_{\text{VHE}} \sim 20$, and most easily by the electron synchrotron process. We find that hadronic processes, both proton-synchrotron and photo-meson, are not efficient enough.

The case for synchrotron emission producing the VHE flare is complicated by the requirement that electrons be accelerated to Lorentz factors of order $\gamma_{\text{e,SYN}} \sim 10^9$ in the face of strong radiative losses. We show that this is only possible in regions where the local electric-to-magnetic fields ratio is $E''/B''_{\perp} \sim 26 \times (\mathcal{D}_{\text{VHE}}/20)^{-1}$. Such a condition can be satisfied within a relativistic magnetic reconnection layer. We consider a model of extreme electron acceleration and focusing applied recently to HE flares in the Crab Nebula. However, in that case, the requirement for the field strength ratio was much weaker, $E''/B''_{\perp} \sim 4$. Applying the LEC to the case of a magnetic reconnection layer, we obtain a

requirement for the reconnecting magnetic field strength: $B''_{\text{VHE}} \gtrsim 130 \text{ G} \times \Omega_e'^{1/2} (\mathcal{D}_{\text{VHE}}/20)^{-3}$. While this value is extremely high for parsec-scale jets, the corresponding magnetic energy density is comparable to $u''_{\text{j,VHE}}$. If the high total jet energy density can be more easily achieved with a high magnetization, then magnetic reconnection is the dissipation mechanism of choice.

Energetic considerations indicate that a substantial fraction of the total jet power, $(L_{\text{j,VHE,GEC}}/L_{\text{j,HE}}) \sim 15\%$, needs to be carried through a tiny fraction of the jet cross section, $(R''_{\text{VHE}}/R'_j)^2 \sim 10^{-5}$. This puzzle of an extreme energy concentration in a parsec-scale jet can be solved in two ways: either the energy focusing is achieved at parsec scales, as in the reconfinement scenario (Section 5.1.4); or it is achieved at much smaller scales and maintained as jet substructure propagating well beyond the BLR (Section 5.1.5). There is a fundamental thermodynamic difference between these two options. In the first case, entropy has to decrease within the jet, and this decrease has to be balanced by entropy transfer to the environment, e.g. via radiative cooling. In the second case, the entropy of the jet substructure could remain constant or even slightly increase. This argument favors a self-collimated jet substructure as the origin of the VHE flare in PKS 1222+216.

ACKNOWLEDGMENTS

This work was partly supported by the NSF grant AST-0907872, the NASA ATP grant NNX09AG02G, and the Polish NCN grant DEC-2011/01/B/ST9/04845.

REFERENCES

- Abdo, A. A., et al., 2010, *Nature*, 463, 919
- Abdo, A. A., et al., 2011, *Science*, 331, 739
- Aharonian, F., et al., 2006, *Science*, 314, 1424
- Aharonian, F., et al., 2007, *ApJ*, 664, L71
- Aharonian, F., et al., 2009, *A&A*, 502, 749
- Albert, J., et al., 2007, *ApJ*, 669, 862
- Albert, J., et al., 2008, *Science*, 320, 1752
- Aleksić, J., et al., 2011, *ApJ*, 730, L8
- Barkov, M. V., Aharonian, F. A., Bogovalov, S. V., Kelner, S. R., Khangulyan, D. V., 2010, arXiv:1012.1787
- Begelman, M. C., Rudak, B., Sikora, M., 1990, *ApJ*, 362, 38
- Begelman, M. C., Fabian, A. C., Rees, M. J., 2008, *MNRAS*, 384, L19
- Beskin, V. S., 2010, *Physics Uspekhi*, 53, 1199
- Boutelier, T., Henri, G., Petrucci, P.-O., 2008, *MNRAS*, 390, L73
- Böttcher, M., Reimer, A., Marscher, A. P., 2009, *ApJ*, 703, 1168
- Bromberg, O., Levinson, A., 2009, *ApJ*, 699, 1274
- Buehler, R., et al., 2011, arXiv:1112.1979
- Celotti, A., Ghisellini, G., 2008, *MNRAS*, 385, 283
- Cerutti, B., Uzdensky, D. A., Begelman, M. C., 2012, *ApJ*, 746, 148
- de Jager, O. C., Harding, A. K., Michelson, P. F., et al., 1996, *ApJ*, 457, 253

- Foschini, L., Ghisellini, G., Tavecchio, F., Bonnoli, G., Stamerra, A., 2011, arXiv:1110.4471
- Ghisellini, G., Tavecchio, F., Chiaberge, M., 2005, *A&A*, 432, 401
- Ghisellini, G., Tavecchio, F., 2008, *MNRAS*, 386, L28
- Giannios, D., Uzdensky, D. A., Begelman, M. C., 2009, *MNRAS*, 395, L29
- Gracia, J., Vlahakis, N., Agudo, I., Tsinganos, K., Bogovalov, S. V., 2009, *ApJ*, 695, 503
- Granot, J., Komissarov, S. S., Spitkovsky, A., 2011, *MNRAS*, 411, 1323
- H.E.S.S. Collaboration, 2010, *A&A*, 520, A83
- Hovatta, T., Valtaoja, E., Tornikoski, M., Lähteenmäki, A., 2009, *A&A*, 494, 527
- Homan, D. C., Kadler, M., Kellermann, K. I., Kovalev, Y. Y., Lister, M. L., Ros, E., Savolainen, T., Zensus, J. A., 2009, *ApJ*, 706, 1253
- Jorstad, S., Marscher, A., Agudo, I., Harrison, B., 2011, arXiv:1111.0110
- Kirk, J. G., 2004, *PhRvL*, 92, 181101
- Komissarov, S. S., Vlahakis, N., Königl, A., Barkov, M. V., 2009, *MNRAS*, 394, 1182
- Komissarov, S. S., 2012, arXiv:1201.3469
- Levinson, A., 2007, *ApJ*, 671, L29
- Lyutikov, M., 2010, *MNRAS*, 405, 1809
- Lyutikov, M., Lister, M., 2010, *ApJ*, 722, 197
- Malmrose, M. P., Marscher, A. P., Jorstad, S. G., Nikutta, R., Elitzur, M., 2011, *ApJ*, 732, 116
- Mannheim, K., 1993, *A&A*, 269, 67
- Meyer, E. T., Fossati, G., Georganopoulos, M., Lister, M. L., 2011, *ApJ*, 740, 98
- Mücke, A., Protheroe, R. J., Engel, R., Rachen, J. P., Stanev, T., 2003, *APh*, 18, 593
- Nalewajko, K., 2010, *IJMPD*, 19, 701
- Nalewajko, K., Sikora, M., 2009, *MNRAS*, 392, 1205
- Nalewajko, K., Giannios, D., Begelman, M. C., Uzdensky, D. A., Sikora, M., 2011, *MNRAS*, 413, 333
- Nenkova, M., Sirocky, M. M., Nikutta, R., Ivezić, Ž., Elitzur, M., 2008, *ApJ*, 685, 160
- O’Sullivan, S. P., Gabuzda, D. C., 2009, *MNRAS*, 400, 26
- Poutanen, J., Stern, B., 2010, *ApJ*, 717, L118
- Pushkarev, A. B., Kovalev, Y. Y., Lister, M. L., Savolainen, T., 2009, *A&A*, 507, L33
- Savolainen, T., Wiik, K., Valtaoja, E., Jorstad, S. G., Marscher, A. P., 2002, *A&A*, 394, 851
- Sikora, M., Begelman, M. C., Madejski, G. M., Lasota, J.-P., 2005, *ApJ*, 625, 72
- Sikora, M., Moderski, R., Madejski, G. M., 2008, *ApJ*, 675, 71
- Sikora, M., Stawarz, L., Moderski, R., Nalewajko, K., Madejski, G. M., 2009, *ApJ*, 704, 38
- Smith, P. S., Schmidt, G. D., Jannuzi, B. T., 2011, arXiv:1110.6040
- Stawarz, L., Aharonian, F., Kataoka, J., Ostrowski, M., Siemiginowska, A., Sikora, M., 2006, *MNRAS*, 370, 981
- Stern, B. E., Poutanen, J., 2008, *MNRAS*, 383, 1695
- Striani, E., et al., 2011, *ApJ*, 741, L5
- Tanaka, Y. T., et al., 2011, *ApJ*, 733, 19
- Tavecchio, F., Ghisellini, G., 2008, *MNRAS*, 386, 945
- Tavecchio, F., Becerra-Gonzalez, J., Ghisellini, G., Stamerra, A., Bonnoli, G., Foschini, L., Maraschi, L., 2011, *A&A*, 534, A86
- Tchekhovskoy, A., Narayan, R., McKinney, J. C., 2011, *MNRAS*, 418, L79
- Uzdensky, D. A., Cerutti, B., Begelman, M. C., 2011, *ApJ*, 737, L40
- Wagner, S., Behera, B., 2010, in 10th HEAD Meeting, Hawaii, BAAS, 42, 2, 07.05